Reflecting AWG by using photonic crystal reflector on Indium-phosphide membrane on silicon platform

Reflecting AWG by Using Photonic Crystal Reflector on Indium-Phosphide Membrane on Silicon Platform

Xuebing Zhang, *Student Member, IEEE*, Jorn Van Engelen, Sander Reniers, Zizheng Cao, *Member, IEEE*, Yuqing Jiao, *Member, IEEE*, and A. M. J. Koonen, *Fellow, IEEE*

***Abstract*— In this letter, a reflection-type arrayed waveguide grating (AWG) (de)multiplexer using high-reflection photonic crystal reflector (PCR) in the Indium-phosphide Membrane on Silicon (IMOS) platform is proposed and experimentally demonstrated for the first time. This reflection-type AWG enables a 35% size-reduced footprint compared with the traditional transmission-type AWG having the same spectral parameters. Considering the realized performance of silicon-nanowire R-AWGs, an acceptable performance (680 × 190 μm^2 size, 6.7-dB loss, and 10-dB crosstalk) is obtained. By using the ultra-small 5.4 × 0.7 μm^2 PCR, merely 1.1-dB power loss higher than the corresponding transmission-type AWG is implemented. The PCR is a standard building block with a reflectivity of >90%. Besides, the length reduction of the arrayed waveguide will contribute to minimize the accumulated phase error in fabrication.**

***Index Terms*— Indium-phosphide membrane on silicon (IMOS) platform, AWG, reflection-type AWG, photonic crystal reflector (PCR).**

I. INTRODUCTION

WITH the rising requirements of higher bit-rate data transport and massive computing, the electronic integrated circuits alone cannot support [1]. In order to deal with these challenges, the photonic integrated circuits has been created using different materials. A popular technology is the Silicon-on-insulator (SOI), which has attracted wide attention and many high-quality photonic devices such as high-speed modulators and photodetectors are implemented [2], [3]. However, due to the indirect bandgap feature of silicon, the integration of optical sources and amplifiers cannot be easily realized on such chips. Several approaches are proposed to solve this problem such as using off-chip light source, designing III-V lasers/amplifier/detectors and coupling light between these devices and silicon waveguides [4]–[6]. However, in monolithic integration, the size of devices on chip is required to be much smaller. Thus the coupling between III–V sections and silicon waveguides is inefficient [7]. To solve these problems, the novel Indium-phosphide Membrane on Silicon (IMOS) platform has been proposed [7]–[9], in which the silicon membrane for waveguide on SOI platforms is replaced by an InP-membrane. Monolithic integration of active and passive components is possible by using a single III–V membrane. This technique can solve many problems such as the coupling between active and passive components and the alignment with respect to the underlying silicon circuit [8]. Moreover, the passive devices such as typical single-mode waveguide (width: 0.4 μm) and waveguide bend (minimum radius: 5 μm) can realize comparable footprint as the ones in SOI platforms, which support very high-density integration. Currently, many passive and active components on IMOS platform have been demonstrated with fully acceptable performance [7]. Fig. 1 describes the cross-section of a standard IMOS passive waveguide. The top is the InP-based membrane photonic layer, in which both IMOS passive waveguides and active lasers/semiconductor optical amplifiers have been fabricated [8]. The standard single-mode waveguide has a width of 400 nm and a thickness of 300 nm. Then divinylsiloxane-bis-benzocyclobutene (DVS-BCB, refractive index = 1.5) is used as the adhesive polymer with a thickness of ∼2 μm. The bottom layer is the substrate (Silicon). The passive waveguide is fabricated by using Electron-beam lithography (EBL) and dry etching technologies.

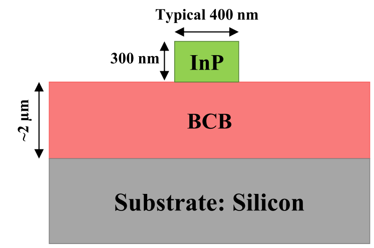

Fig. 1. Cross section of a standard IMOS passive waveguide.

IMOS platform is aiming at realizing monolithic integration of active and passive components in a single InP membrane. As the important (de)multiplexer, arrayed waveguide grating (AWG) is necessary for a system design

Manuscript received February 12, 2019; revised March 31, 2019; accepted May 12, 2019. Date of publication May 15, 2019; date of current version June 12, 2019. This work was supported in part by the European Research Council in Advanced Grant project BROWSE and Proof-of-Concept Project BROWSE+, in part by the NWO Zwaartekracht Program on Integrated Nanophotonics, in part by the National Natural Science Foundation of China (NSFC) under Grant 61575186 and Grant 61635001, in part by the Open Fund from the State Key Laboratory of Advanced Optical Communication Systems Networks, China, and in part by the NWO China Exchange Programme under Grant 530-5CDP06. *(Corresponding authors: Zizheng Cao; Yuqing Jiao.)*

The authors are with the IPI Institute, Eindhoven University of Technology, 5600 MB Eindhoven, The Netherlands (e-mail: z.cao@tue.nl; y.jiao@tue.nl).

Color versions of one or more of the figures in this letter are available online at http://ieeexplore.ieee.org.

Digital Object Identifier 10.1109/LPT.2019.2917147

on-chip [10]. Especially the smaller footprint reflection-type AWG (R-AWG) can further increase the density of integration. So far no R-AWG is reported except a similar InP-membrane-based T-AWG with measured insertion losses (IL) of 6 dB and −10-dB cross-talk [11]. In contrast, SOI R-AWGs have been successfully fabricated and the measured values of footprint, insertion loss and crosstalk are 134 μm × 115 μm, 3-4 dB and −12 dB [12], 530 μm × 230 μm, 3 dB and −20 dB [13], 950 μm × 350 μm, ~3.5 dB and ~−8 dB [14], 850 μm × 170 μm, 7 dB and −8 dB [15], respectively.

In this letter, an R-AWG (de)Multiplexer using high reflection photonic crystal reflector (PCR) on the IMOS platform is proposed and experimentally demonstrated for the first time. This R-AWG enables a 35% size-reduced footprint at a cost of 1.1dB extra loss compared with the traditional transmission-type AWG (T-AWG) having the same spectral parameters. Compared with silicon-nanowire R-AWGs, an acceptable performance (680 μm × 190 μm, 6.7-dB loss, and 10-dB crosstalk) is obtained. The ultra-small 5.4-by-0.7 μm^2 PCR can realize >90% reflectivity. Besides, the length reduction of the arrayed waveguide will contribute to minimize the accumulated phase error caused by the variation-sensitive waveguides.

II. Operation Principles

Fig. 2 (a) explains the working principle of R-AWG. In terms of the layout, a T-AWG is usually symmetrical such as the architecture shown here. The input light will go through two identical half-layout. Thus the same function can be achieved by using the half layout and reflectors at the end of the arrayed waveguides as presented in the right part of Fig. 2 (a). Because the light in R-AWG passes the same structure twice, which is logically equivalent to T-AWG. Thus the T-AWG allows a more flexible adjustment of grating order [12]. Fig. 2 (b) shows the schematic configuration of the proposed IMOS-based R-AWG (de)multiplexer. This device is fabricated in one of the IMOS Multi-Project-Wafer (MPW) runs carried out in the IPI-TU/e (Institute for Photonic Integration, Eindhoven University of Technology) [7]. The R-AWG contains 8 input/output waveguides, in which anyone can be selected as the input port. The vertically-coupled light via a surface grating will be firstly fed into a Fan-in area which is composed by a taper array. The Fan-in architecture helps increase the power coupling efficiency from a single-mode rectangle waveguide (400-nm width) to the slab waveguide, which is called the free propagation region (FPR). Then the light will be coupled to a Fan-out structure followed by a plurality of arrayed waveguides, waveguide bends, and the PCRs. Finally, a taper is used to minimize the end reflection of the transmission light. The radius of the bending is 10 μm. In fact, the waveguide bends can be removed and thus it contributes to minimize the accumulated phase error [13]. Here, the bends are reserved to obtain the contributions only from PCRs in the comparison in Fig. 4 (a).

The key component realizing the R-AWG is the ultra-small PCR which is a standard building block with very high stability in IMOS platform [16]. As presented in Fig. 2 (b), the size of the PCR is 0.7-μm wide and 5.4-μm long, with

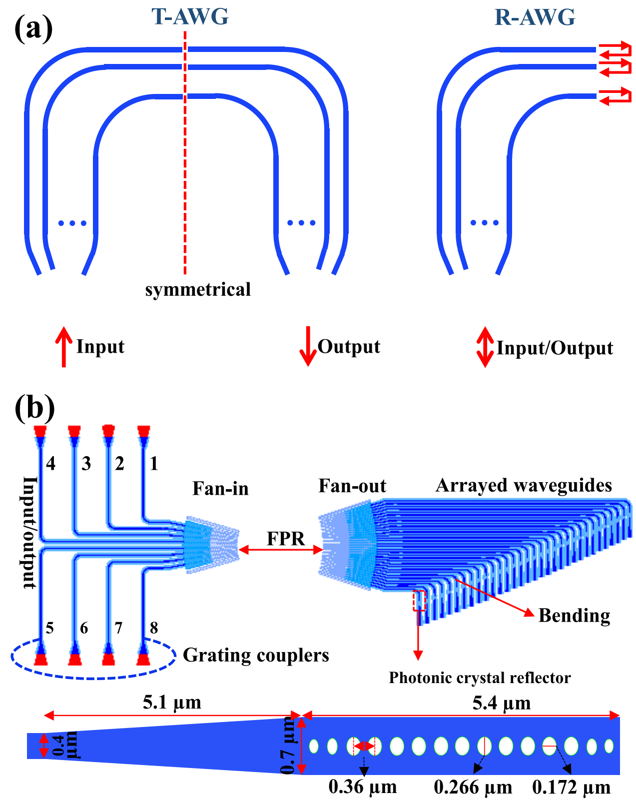

Fig. 2. (a) Layout comparison between T-AWG and R-AWG; (b) The schematic configuration of the proposed IMOS-based R-AWG (de)multiplexer. FPR: free propagation region.

15 deep-etched holes along the central axis. The inter-hole spacing is set as 0.36 μm and the minor and major axis diameters of the ellipse-shaped holes are 0.266 μm and 0.172 μm, respectively. At each end, the hole is slowly getting smaller in order to reduce the scattering at the interface (from the waveguide to PCR). The period numbers of holes is required to obtain a high reflection. In our design, the light is coupled into the proposed PCR (width: 0.7 μm) from a typical single-mode waveguide (0.4 μm), thus a simple linear taper is employed in between to suppress radiation modes. The similar PCRs in the IMOS platform have been reported [8]–[17] as high reflectivity mirrors for laser cavities. The simulation results using Lumerical 3 dimensional (3-D) finite-difference time-domain (FDTD) method (mesh accuracy is set as 6) are depicted in Fig. 3. The reflectivity can be >90% in a broad wavelength range of >200 nm, especially in the C band (1530 nm-1565 nm), >95% light can be reflected. The detailed experimental analysis on 11-/8-/6-/0-hole photonics crystal reflectors is done in [16]. In this work, two methods are used to measure the reflectivity, in which the real reflectivity is approximated with high accuracy. In our design, a 15-hole reflector is used, which, in theory, has an even higher reflectivity than 11-hole reflector. However, due to the extremely low signal transmission through the 15-hole reflector, the accurate measurement of the reflectivity is not easy using the methods in [16]. In order to avoid an inaccurate data, only the simulation performance is shown in this letter. The real reflectivity can be estimated through [16].

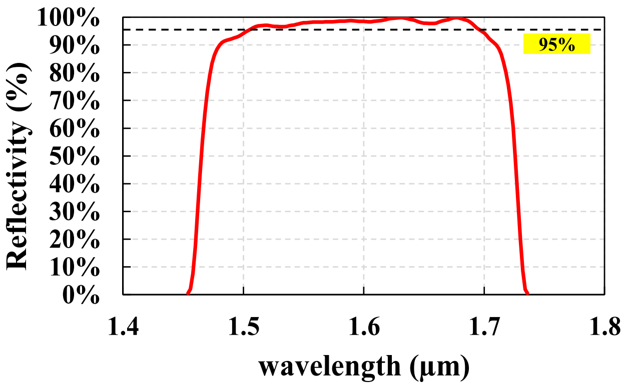

Fig. 3. The calculated reflectivity of the reflecting structure (including the photonic crystal reflector, taper and the single mode waveguide).

III. Experimental Results and Discussions

To demonstrate the effectiveness of the designed IMOS R-AWG by using PCRs, a set of T-AWG and R-AWG with the same spectral parameters are fabricated on the same chip. In both designs, the end spacing between adjacent input/output waveguides is 3.7 μm and the length of FPR is 130 μm. The end separation and the number of arrayed waveguides are 2.5 μm and 32 respectively. In terms of frequency response, the designed central wavelength is set as 1550 nm with 4-nm channel spacing and 32-nm free spectrum range (FSR). Fig. 4 (a) presents the fabricated T-AWG and R-AWG on the InP-membrane. It is obvious that the size of the R-AWG (129200 μm^2) has been reduced compared with 8-by-8 T-AWG (199650 μm^2). By halving the FPR area and the length of the arrayed waveguides, 35% of the size is reduced. The waveguides with a grating coupler on each end next to the AWGs is used to calibrate the coupling loss of the grating couplers. In the T-AWG, because the 4th input waveguide is designed for other application, the fifth input waveguide is selected as the input port of our measurement. While, in R-AWG, the 1st and 4th input waveguides are the input ports. Fig. 4(b) describes the measurement of the reflection-type AWG. The input/output cleaved single mode fibers are aligned vertically and the coupling angle is about 9.5 degree. Due to the limitation of the measurement system, only 5th-8th input/output waveguides are measured according to the two input ports.

Fig. 5(a) shows the measurement setup. An amplified spontaneous emission light source that covers the whole C-band (1530 nm to 1565 nm) is polarization-filtered by a polarization beam splitter (PBS). The polarization state of the output light from the light source is further aligned to transverse electric (TE) polarization by using a polarization controller (PC) and is fed into the chip measurement system: two vertically coupling single-mode fibers and the device under tested (DUT). An optical spectrum analyzer (OSA) is utilized to measure the frequency response of the AWGs. The normalized amplitude response of the transmission-type AWG using 5th waveguide as the input port is depicted in Fig. 5(b). The power loss is 5.6 dB (including the input and output waveguides) with acceptable 3-dB power imbalance between the central and edge channels. The measured

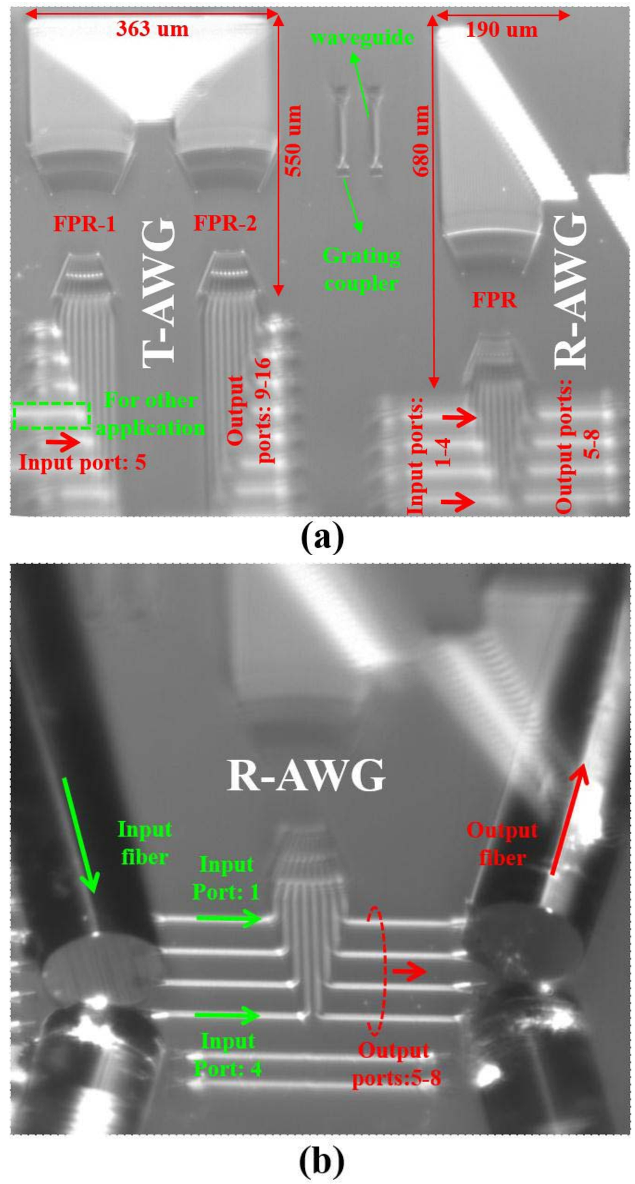

Fig. 4. (a) Photo of the fabricated IMOS-based T-AWG and R-AWG (de)multiplexers. (b) Photo of the measurement of the designed R-AWG using vertically-aligned fibers.

channel spacing (4 nm) perfectly matches the designed value. While the FSR experiences 1-dB increase from the designed 32 nm to the fabricated 33 nm. The inter-channel crosstalk is around −11.4 dB. The size-reduced R-AWG implements the same 4-nm channel spacing, 3-dB output amplitude variation, and the 10-dB crosstalk. Only 1.1-dB extra loss is introduced after the fabrication. Because the input port number is 4 (5 in T-AWG), there is a wavelength blue shift of 4-nm (one channel spacing) compared with the T-AWG's response. The response is more noisy than the relative T-AWG. One possible contribution to the response is the higher-order mode excitation due to the nonvertical sidewalls in the fabricated photonic crystal reflector. When the input port is changed to the first, the cyclic response can be observed as shown in Fig. 5(d). Usually, the power loss increases with the spacing increase off the central input waveguide. Here the loss is

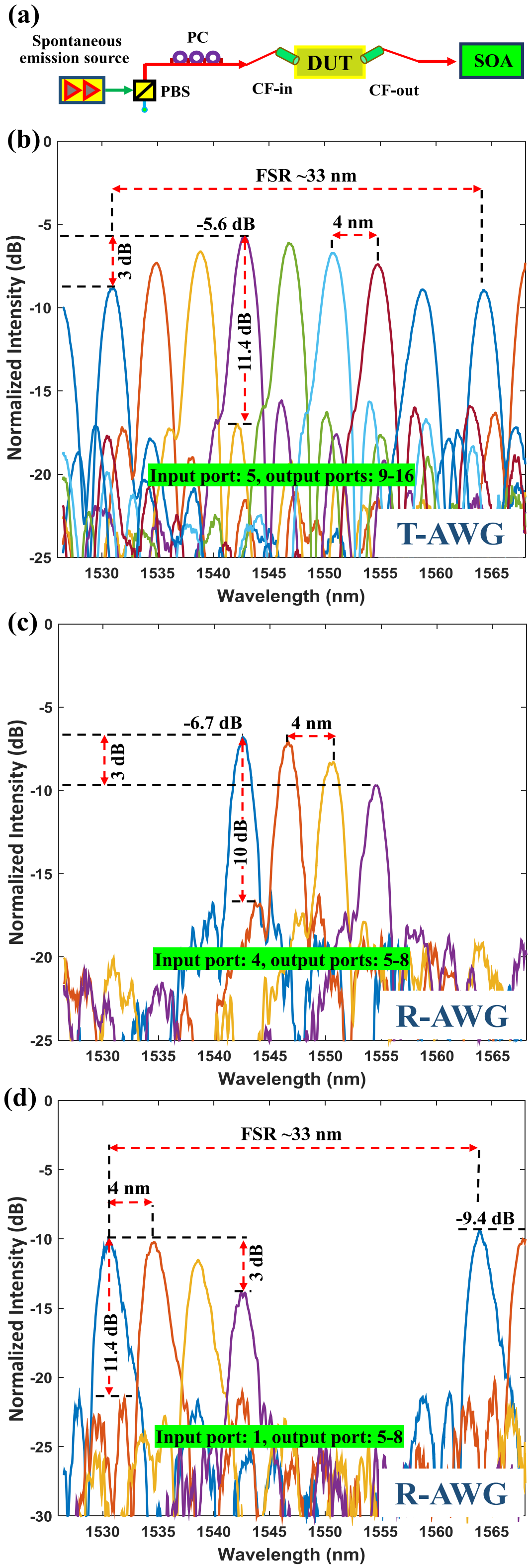

Fig. 5. (a) The measurement system; (b) the measured 5th-port-input T-AWG response; (c) the measured 4th-port-input R-AWG response; (d) the measured 1st-port-input R-AWG response. PBC: polarization beam splitter; PC: polarization controller; CF-in/out: cleaved input/output fibers; DUT: devices under test; OSA: optical spectrum analyzer.

9.4 dB with 2.8-dB increase. The wavelength blue shift is 12 nm and the cross talk is 11.4 dB. The channel spacing (4 nm), the power uniformity (3 dB) and the FSR (33 nm) are all maintained. The R-AWG proves an effective way of reducing footprint with very limited power cost.

IV. Conclusion

In conclusion, the reflection-type AWG (de)Multiplexer using ultra-small PCRs (5.4-by-0.7 μm^2) on the IMOS platform is designed and experimentally demonstrated. This R-AWG enables a 35% size-reduced footprint and only 1.1-dB extra loss without impacting the crosstalk performance compared with the traditional transmission-type AWG having the same spectral parameters. The length reduction of the arrayed waveguide will contribute to higher-density photonic integrated circuits in the IMOS platform.

References

[1] L. Liu, G. Roelkens, J. V. Campenhout, J. Brouckaert, D. V. Thourhout, and R. Baets, "III–V/silicon-on-insulator nanophotonic cavities for optical network-on-chip," *J. Nanosci. Nanotechnol.*, vol. 10, no. 3, pp. 1461–1472, 2010.

[2] B. Jalali and S. Fathpour, "Silicon photonics," *J. Lightw. Technol.*, vol. 24, no. 12, pp. 4600–4615, Dec. 2006.

[3] S. Assefa, F. Xia, and Y. A. Vlasov, "Reinventing germanium avalanche photodetector for nanophotonic on-chip optical interconnects," *Nature*, vol. 464, no. 7285, pp. 80–85, 2010.

[4] Y. Vlasov, W. M. J. Green, and F. Xia, "High-throughput silicon nanophotonic wavelength-insensitive switch for on-chip optical networks," *Nature Photon.*, vol. 2, no. 4, pp. 242–246, 2008.

[5] D. V. Thourhout *et al.*, "A photonic interconnect layer on CMOS," in *Proc. 33rd Eur. Conf. Exhib. Opt. Commun.*, Sep. 2007, pp. 1–2.

[6] A. W. Fang, H. Park, O. Cohen, R. Jones, M. J. Paniccia, and J. E. Bowers, "Electrically pumped hybrid AlGaInAs-silicon evanescent laser," *Opt. Express*, vol. 14, no. 20, pp. 9203–9210, 2006.

[7] J. J. G. M. van der Tol *et al.*, "Indium phosphide integrated photonics in membranes," *IEEE J. Sel. Topics Quantum Electron.*, vol. 24, no. 1, pp. 1–9, Jan./Feb. 2018.

[8] V. Pogoretskiy, P. J. van Engelen, J. J. G. M. van der Tol, and Y. Jiao, "Towards a fully integrated indium-phosphide membrane on silicon photonics platform," *Proc. SPIE* vol. 10823, Oct. 2018, Art. no. 1082308.

[9] J. van der Tol *et al.*, "Photonic integration in indium-phosphide membranes on silicon (IMOS)," *Proc. SPIE*, vol. 8988, Mar. 2014, Art. no. 89880M.

[10] M. K. Smit and C. Van Dam, "PHASAR-based WDM-devices: Principles, design and applications," *IEEE J. Sel. Topics Quantum Electron.*, vol. 2, no. 2, pp. 236–250, Jun. 1996.

[11] M. Takenaka, M. Yokoyama, M. Sugiyama, Y. Nakano, and S. Takagi, "InGaAsP photonic wire based ultrasmall arrayed waveguide grating multiplexer on Si wafer," *Appl. Phys. Express*, vol. 2, no. 12, Nov. 2009, Art. no. 122201.

[12] D. Dai, X. Fu, Y. Shi, and S. He, "Experimental demonstration of an ultracompact Si-nanowire-based reflective arrayed-waveguide grating (de)multiplexer with photonic crystal reflectors," *Opt. Lett.*, vol. 35, no. 15, pp. 2594–2596, 2010.

[13] K. Okamoto and K. Ishida, "Fabrication of silicon reflection-type arrayed-waveguide gratings with distributed Bragg reflectors," *Opt. Lett.*, vol. 38, no. 18, pp. 3530–3533, 2013.

[14] B. Gargallo *et al.*, "Reflective arrayed waveguide gratings based on Sagnac loop reflectors with custom spectral response," *Opt. Express*, vol. 22, no. 12, pp. 14348–14362, 2014.

[15] J. Zou, T. Lang, Z. Le, and J. He, "Ultracompact silicon-on-insulator-based reflective arrayed waveguide gratings for spectroscopic applications," *Appl. Opt.*, vol. 55, no. 13, pp. 3531–3536, 2016.

[16] S. Reniers, J. van Engelen, K. Williams, J. van der Tol, and Y. Jiao, "Waveguide photonic crystal reflectors on InP-membranes-on-silicon," in *Proc. 21st Eur. Conf. Integr. Opt.*, Apr. 2019, pp. 1–3.

[17] A. H. Rodriguez, V. Pogoretskii, P. J. van Veldhoven, A. Fiore, D. Heiss, and M. K. Smit, "Densely integrated membrane-based nano-beam lasers for optical interconnects," in *Proc. 20th Annu. Symp. IEEE Photon. Benelux Chapter*, vol. 26, Nov. 2015, p. 27.